IOP Conf. Series: Materials Science and Engineering **124** (2016) 012084 doi:10.1088/1757-899X/124/1/012084

Application of a Lamb waves based technique for structural health monitoring of GFRP undercyclic loading

A Eremin[1, 2], A Byakov[1, 2], S Panin[1, 2], M Burkov[1, 2], P Lyubutin[1, 2] and R Sunder[3]
[1] Institute of Strength Physics and Materials Science of the Siberian Branch of the Russian Academy of Sciences, 2/4, Akademicheskiy ave., Tomsk, 634021, Russia
[2] Tomsk Polytechnic University, 30, Lenina ave., Tomsk, 634050, Russia
[3] Bangalore Integrated System Solutions Ltd, 497E 14th Cross, 4th Phase, Peenya Industrial Area, Bangalore, 560058, India

E-mail: eremin_av@bk.ru

Abstract. A Lamb wave based ultrasonic technique as well as optical image characterization was utilized to estimate a current mechanical state of glass fiber reinforced polymers (GFRP) under cyclic tension. The ultrasonic acoustic method was applied in a 'pitch-catch' mode using piezoelectric transducers adhesively bonded onto a specimen surface. Numerical evaluation of acoustic data was performed by calculating two informative parameters: maximum of amplitude of the received signal and variance of signal envelopes. Optical images were registered and then analysed by calculating Shannon entropy that makes it possible to characterize changing of GFRP specimen translucency. The obtained results were treated in order to find out the relation between the current mechanical state of a specimen and informative parameter values being computed from the acoustic and optical signals.

1. Introduction

Recently advanced composite materials such as glass/carbon fiber reinforced polymers (FRP) have found wide use as structural materials for various engineering applications [1]. The advantages of glass/carbon FRPs over conventional metallic materials results in wide-spread replacement of metals in civil engineering, wind energy, shipbuilding, aerospace and etc. However, due to the lack of ductility the structures made of these composites exhibit brittle (catastrophic) failure and require the application of higher safety factors during design and accurate inspections throughout the entire operating life. Since FRPs tend to find wide spread occurrence the research and development of new methods of their inspection is a relevant task.

The problem of identification of flaws and damages long before failure as well as performing condition-based maintenance requires the information about the structure's mechanical state, which can be provided by Structural Health Monitoring (SHM) systems. Lamb waves techniques are popular for implementation in SHM [2] due to their low attenuation that allows covering large inspection areas [3] and ensures the possibility of detecting damages of various sizes as well as evaluating of the changes of mechanical properties of the material.

However, Lamb waves have a multi-mode dispersive nature, thus the raw captured (acoustic sensing) data are quite complex for interpretation [4]. When a wave is transmitted from an actuator to a receiver a lot of different wave modes appear and each of them propagates with a unique through

thickness displacement and stress profile [5]. It might be beneficial to use multi-mode Lamb waves with a different wavelength and, thus, with different sensitivity to defects.

Lamb waves could be generated using piezoelectric actuators or high energy laser impulse and then sensed by various techniques such as optical fiber Bragg cells, non-contact laser vibrometry or piezoelectric sensors. The last one seems to be one of the most versatile technique due to the possibility of simultaneous signals transmitting and receiving. In doing so, large areas could be covered by a network of sensors.

The aim of the present study is development and testing of the Lamb wave based technique combined with the optical method for estimation of the state of glass fiber reinforced polymer specimens under fatigue tests.

2. Methods and materials

Specimens with chamfered tabs (Figure 1) were tested under fatigue conditions with an equal strain ratio but different maximum strains (0.69 %, 0.77 % and 0.85 %). Specimens were made from E-glass fibers with a polyester matrix. A middle layup [0°] was additionally covered by two surface layers oriented at[+45°,-45°].

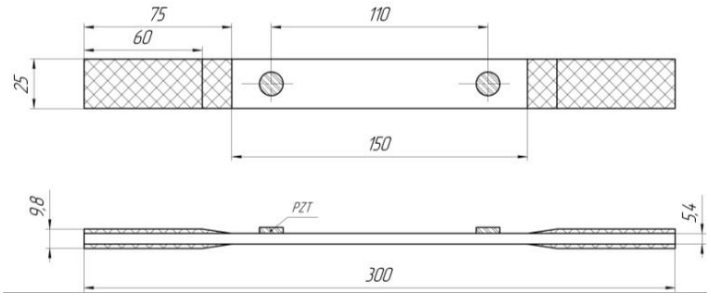

Figure 1. A specimen's design.

During experiments two types of data were acquired: digital optical images of the specimen's surface and acoustic wave signals after their propagation along the specimen area located between two PZT transducers. In doing so one piezo transducer plays a role of an actuator (generates ultrasonic waves) and the other PZT is a sensor (receives acoustic waves). When acoustic disturbance propagates through the bulk specimen it interacts with nearly all large enough heterogeneities and scatters onto those defects which size is larger than or equal to the wave length. These interactions and scatterings give rise to changes of the acoustic response of the material: propagation velocity, amplitude, waveform, spectrum and etc. Detailed analyses of changes taking place in a signal provide the information about various types of defects and make the internal structure reconstruction possible.

Photos were captured by digital camera Canon EOS 750D with resolution of 5184×3456 pixels. Acoustic waves were generated by arbitrary waveform generator AWG-4105 with the amplitude of 10 V. Signal sensing was conducted by USB oscilloscope Handyscope HS4 with the sampling rate of 5 MHz and with the 12 bit resolution. AW1E12G-190EFL1Z (a 9 mm disc with thickness of 0.19 mm) piezoelectric transducers were used for acoustic wave transmitting and receiving. The signal from the generator was recorded by the 1st channel of HS4 to be used as the timing reference to automate the experimental procedure by triggering the data acquisition. The registered signals were processed using a 10…800 kHz band-pass filter.

Figure 2 illustrates the initial signal waveform – 5 cycles of sine modulated by the Hanning window. Such shape of the signal was chosen due to a relatively long duration, bell curve spectral properties and possibilities of recognizing different wave packets in a received signal.

Acoustic and optical data were acquired after every 1000 cycles in the automatic mode. At the same time cyclic loading was not interrupted. The disadvantage of such technique is variation of the mechanical state from one reading to another, since capturing was performed under different values of

applied loads. Figure 3 illustrates the fact that cyclic loading causes changes in the acoustic signal wave form and a specimen visual appearance.

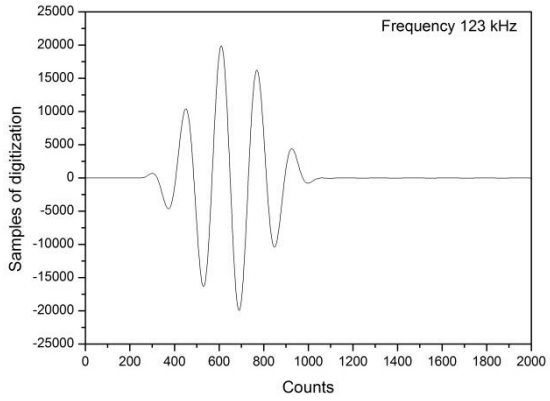

Figure 2. A generated signal waveform (5 cycles of sine modulated by the Hanning window)

Subsurface delamination progresses and it changes specimen transparency, which emerges as white areas being visible on the surface. Damage formation is reflected in the acoustic signal by its amplitude decline; then the signal changes its waveform (which is related to overlapping of different wave packets received, arrival of reflected packets and their interference). Due to the overall phenomena it is possible to evaluate changes in integral properties of the material, predict residual life time or estimate the defect location, size and type.

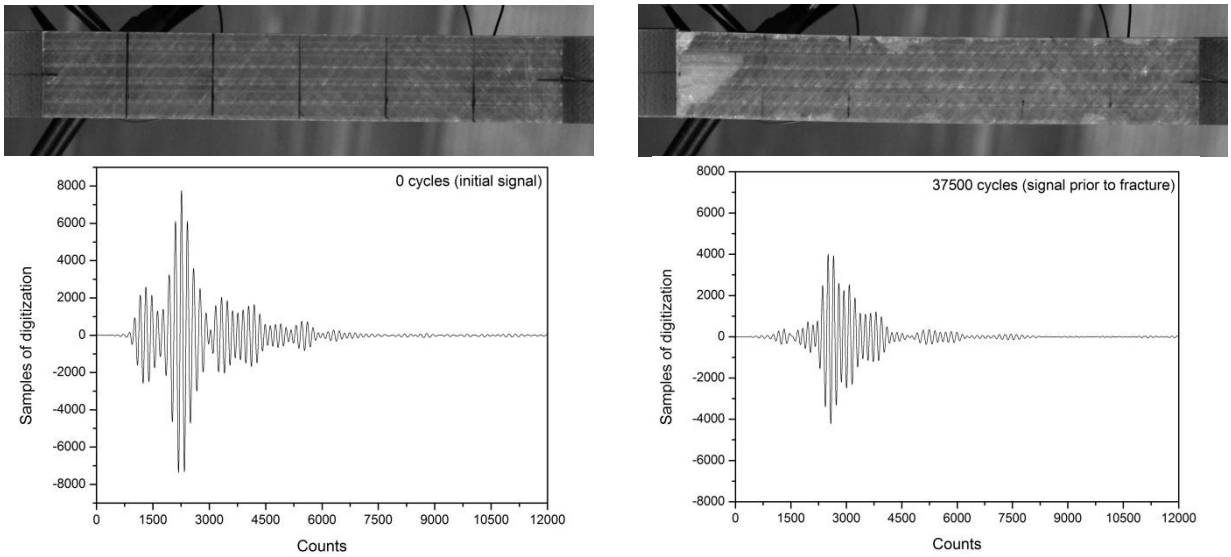

Figure 3. Optical images and acoustic signals waveforms of a GFRP specimen in two states: undeformed (left) and prior to fracture (right)

Recorded data were numerically analyzed and each data acquisition point corresponded to computed values, which characterize the acoustic signal and a surface image. Thus information on the material state becomes available in terms of quantity. One of the calculated parameters used for characteristic of acoustic signals is variance (the 2nd central moment) between signals envelopes. It can be calculated by equation (1).

$$\mu_2 = D[X] = M[(X - m_x)^2] = \sum_{i=1}^{n} (x_i - m_x)^2 \quad (1)$$

where x_i – difference between two signal envelopes, m_x – expected value ofx_i.

A parameter, which characterizes optical images, is Shannon Entropy (or information entropy) which iscalculated usingequation (2).

$$H = -\sum_{i=0}^{255} \frac{HIST_i}{255} \log_2 \frac{HIST_i}{255} \quad (2)$$

i – pixel intensity value (brightness), $HIST_i$ – sum of pixels of the whole image with an*i*-value of intensity (it is an*i*-value of the image histogram, i. e. brightness distribution over the digital image).

Specimens were tested in slightly distinct initial conditionsdue to experimental procedure scattering induced by the influence of non-vertical alignment of the specimen in grips, some variation in the ultrasonic sensor location, etc. Also, since the distance between PZTs varies from one specimen to another it was necessary to normalize all calculated parameters (relative to a maximum value) as well as the number of cycles. It allows overcoming specimen inequalities and compensating them.

Before the beginning of systematic experimental studies it was necessary to determine the optimal frequency for acoustic wave sounding. For this purpose the frequency range from 10 kHz to 500 kHz was passed through (scanned) and a sensor response was measured in units of spectrum power (Figure 4). The optimum frequencies for this type of piezo-transducers were selected to be equal to 123 kHz and 243 kHz.The corresponding acoustic wave velocities andwavelengthsarepresented in the table 1.

Table 1. Estimated velocity and wavelength of Lamb waves.

Frequency	Frequency-thicknessproduct, MHz·mm	Symmetric - S_0 mode		Antisymmetric - A_0 mode	
		Velocity, m/s	Wavelength, mm	Velocity, m/s	Wavelength, mm
123 kHz	0.66	≈3900	31	≈1800	14
243 kHz	1.31	≈3700	15	≈2400	10

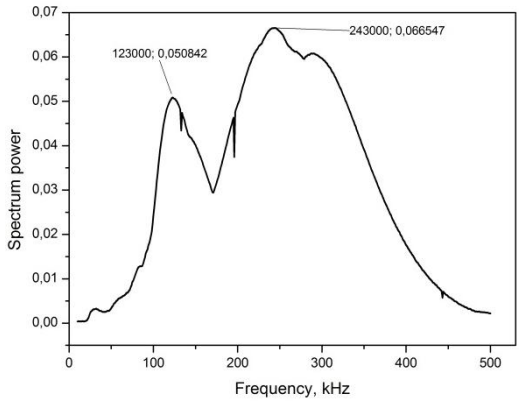

Figure 4. An amplitude-frequency diagram attained in the process of optimum acoustic sounding frequencies finding.

3. Results and discussion

Experiments were performed with the use of 9 specimens (3 specimensof the same type for each strain value). In order to illustrate the most general features and properties, the results for only one specimen from each group are presented in the paper.

Figure 5represents the normalized amplitude of the acoustic signal versus the life time gained during fatigue experiments with three specimen types with various values of maximum strain in a cycle (0.85 %, 0.77 % and 0.69 %).The left plot (a) shows the results when acoustic signal frequency was 123 kHz and the right one (b) – 243 kHz.

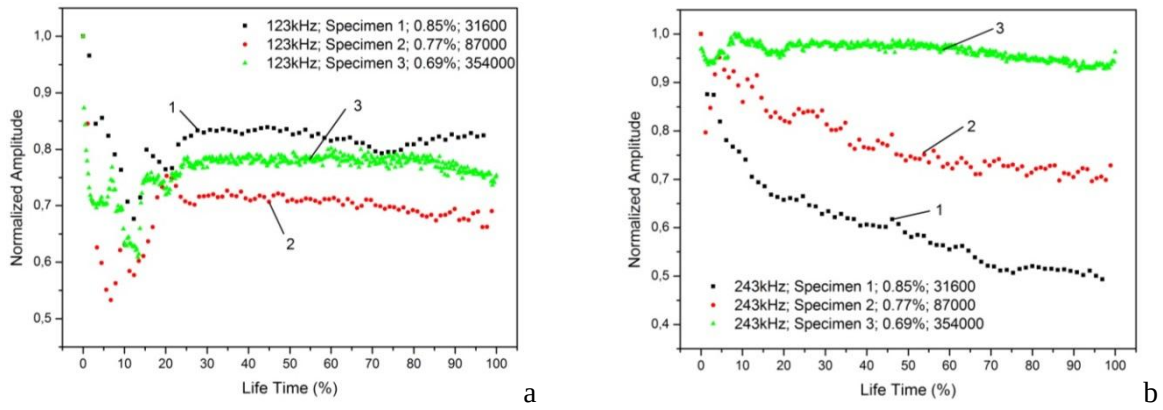

a b

Figure 5. The dependence of normalized signal amplitude versus specimen life time. Specimen 1 – 0.85 %, 31600 cycles; Specimen 2 – 0.77 %, 87000 cycles; Specimen 3 – 0.69 %, 354000 cycles. Frequency of scanning signal: 123 kHz (a) and 243 kHz (b).

As it is seen in Figure 5 (b) the maximum strain value exerts some influence onto the behaviour of acoustic signalsand it depends on the frequency of the acoustic wave. In case of low frequency (123 kHz), which has alarger wavelength and, therefore, lower sensitivity to damages, the dependences do notexhibit any clear correlations between maximum cyclic strain and curve shapes. Whereaswith higher frequency (243 kHz) the wavelength is twice smaller and has higher perceptibility. The latest feature of the acoustic wave stimulatesan increased amplitude response tovariations ofmaximum strains in a cycle. It should be mentioned that the A_0 mode is more informative under signal processing, since the amplitude of the A_0 mode is much higher than that of the S_0 mode. Plots ofthe responses to the high frequency signalshow the downward trendexcluding the first 10 % of life time where some abrupt jumps and drops are registered. The higher is the strain value of appliedload,thesteeperisthe curve of the amplitude-frequency response.

The second parameter of acoustic signals that was computed in order to characterize the specimens' state was variance between two signal envelopes. The dependences of the varianceson the life time are presented in Figure 6.

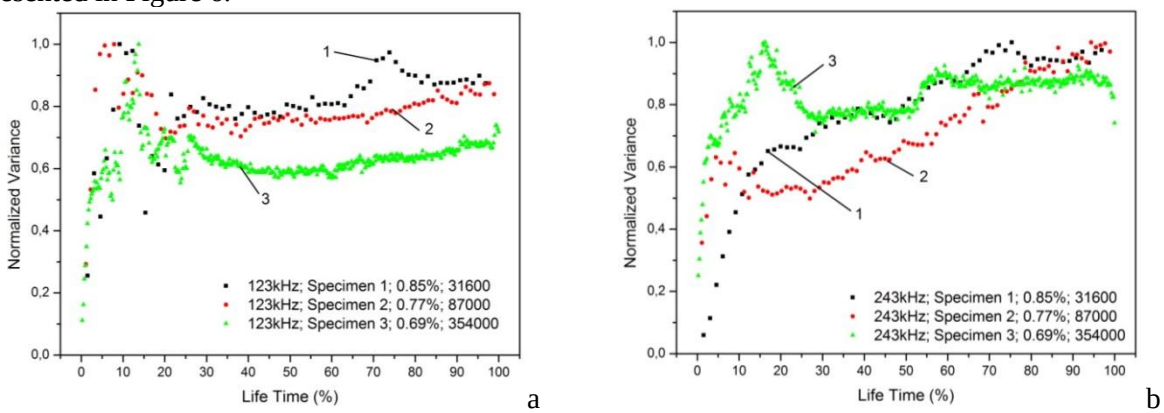

a b

Figure 6. Plots of normalized variance of the acoustic signal versusthe life time for 3 specimens with different strains in a cycle; Specimen 1 – 0.85 %, 31600 cycles; Specimen 2 – 0.77 %, 87000 cycles; Specimen 3 – 0.69 %, 354000 cycles. Frequency of scanning signal: 123 kHz (a) and 243 kHz (b).

Plots characterizing the computed values of the variance for low frequency signalsdepict abrupt rises and drops of the parameter value in presence of the clear upward trend. The latter is a characteristic feature from the beginning of testing and till 20 % of life time. The reason of such behaviour is related to processes of damage formation occurring at the first stage of the fatigue tests. The above mentioned assumption agrees with the optical data, shown in Figure 7. It is seen that after

20 % of life time curves exhibit the smooth trend.The values of variance forthe scanning signal of 243 kHz indicate a sharp increase of the parameter during the first 15 % of life time and then possesses a gradual growth. After 60 % of life time three curves ofthe parameters values tend to intersect.

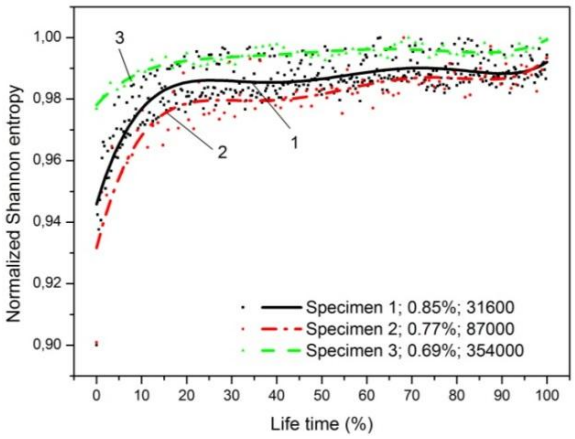

Figure 7. A normalized Shannon entropy (gained from the image processing) dependence on the life time for three specimens with different strains: 0.85 %, 0.77 % and 0.69 %

The results for the optical datacomputationare presented in Figure 7 that indicatesthe dependenceof Shannon entropy for three specimens with a large scattering of the data (smoothed by polynomialfitting and shown by a solid curve) due to imperfection of the image capturing procedure.The analysis of the graphs allows concludingthat the optical transparency suddenly changes after 1000 cycles due to nucleation of micro cracks, loss of adhesion between matrix and fibersas well as delamination. At the last stage of cyclic testing internal changes in the specimens do not substantially influence the optical transparency. Thus, the specimen failure happens without pronounced evidences that might be extracted from the analysis of this parameter.

4. Conclusion

By summarizing the obtained results it is possible to conclude that the combination of the optical and acoustic data analyses provides more comprehensive and robust results for material state characterization for SHM purposes and a condition based maintenance paradigm. An acoustic technique acquiresthe information about the integral mechanical state of a specimensince wave propagation is highly influenced by the specimen stiffness. On the other hand,optical images providethe visualization of cracks and delaminationand allow for location of visible damages. The optical images also provide better sensing of the material structure degradation at first stages of cyclic loading.

A low frequency (123 kHz) ultrasonic inspection does not provide satisfactoryand reliable results fora precise estimation of the material mechanical state, whereas high frequency (243 kHz) seems to be perspectivein theevaluation of residual operating time in future application in the SHM technique. The optical image analysis performed via calculation of theShannon entropy informative parameter clearly indicatesthe structure degradation processes up to 30% of life time,but afterwards itretainsthe value nearly constant up to 90% of life time. Just before fracture the value startsa slow increase.

Prospects of the current investigation arerelated to the following directions of study: a) improvement of data acquisition, processing methodology and techniques, b) development ofthe damage index, which is based on the combination of informative parameters extracted from optical and acoustic signals and c) development of the algorithms for determination of residual operating time and failureprediction.

References

[1] Gand A, Chan T, Mottram J 2013 Civil and structural engineering applications, recent trends, research and developments on pultruded fiber reinforced polymer closed sections *A review. Frontiers of Structural and Civil Engineering* **7** Issue 3 pp 227-244;
[2] Raghavan A, Cesnik C 2007 Review of guided-wave structural health monitoring *Shock Vib. Dig*. **39** pp 91-114;
[3] Carandente R, Cawley P 2012 A method to estimate the size of corrosion patches with guided waves in pipes *AIP Conf. Proc.* **1430** pp 1929-1936;
[4] Miller C, Hinders M 2014 Classification of flaw severity using pattern recognition for guided wave-based structural health monitoring *Ultrasonics* **54** pp 247-258;
[5] Rose J 1999 Ultrasonic Waves in Solid Media *Cambridge University Press*.